Applied Surface Science 357 (2015) 1343–1354

Contents lists available at ScienceDirect

Applied Surface Science

journal homepage: www.elsevier.com/locate/apsusc

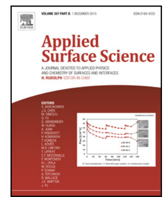

Effect of the Si content on the microstructure of hard, multifunctional Hf–B–Si–C films prepared by pulsed magnetron sputtering

Minghui Zhang[a], Jiechao Jiang[a], Pavel Mareš[b], Jiři Houška[b], Jaroslav Vlček[b], Efstathios I. Meletis[a,*]

[a] Department of Materials Science and Engineering, The University of Texas at Arlington, Arlington, TX 76019, USA
[b] Department of Physics and NTIS European Centre of Excellence, Univerzitni 8, University of West Bohemia, 306 14 Plzeň, Czech Republic

ARTICLE INFO

Article history:
Received 22 July 2015
Received in revised form
25 September 2015
Accepted 29 September 2015
Available online 3 October 2015

Keywords:
Hard coatings
Pulsed magnetron sputtering
High-resolution transmission electron microscopy
X-ray photoelectron spectroscopy
Electron diffraction

ABSTRACT

Pulsed magnetron sputtering in pure Ar was used to deposit multifunctional Hf–B–Si–C films on (0 0 1) silicon substrates using a single B_4C–Hf–Si target. The effect of Si content in the microstructure evolution of the films was studied by X-ray photoelectron spectroscopy, X-ray diffraction, electron diffraction and high-resolution transmission electron microscopy. Hf–B–Si–C films with a chemical composition in at% $Hf_{27}B_{57}C_8$, $Hf_{23}B_{55}Si_2C_{11}$, $Hf_{22}B_{54}Si_9C_9$ and $Hf_{21}B_{28}Si_{35}C_7$, respectively were produced using a fraction of 0%, 1%, 7.5% and 30% Si in the target erosion area. The $Hf_{27}B_{57}C_8$ film is composed of hexagonal HfB_2 nano-columnar structures (~50–60 nm long, and ~5–10 nm wide). The nano-columnar structures exhibit a preferred orientation with the (0 0 1) tilted ~30° away from the film surface. The $Hf_{23}B_{55}Si_2C_{11}$ film consists of finer HfB_2 nanocrystal columnar structures (~20–30 nm long and <5 nm wide) concealed by ~1 nm thick amorphous boundaries. All nano-columns are uniquely oriented with the (0 0 1) parallel to the film surface. The $Hf_{22}B_{54}Si_9C_9$ film consists of refined nano-needle structures (~2–3 nm wide) composed of randomly oriented multi nanocrystals and the $Hf_{21}B_{28}Si_{35}C_7$ film consists of a nanocomposite structure of HfB_2 nanocrystals (1–2 nm) embedded in an amorphous matrix. The incorporation of Si into the films results in microstructural refinement and promotes the formation of an amorphous structure. As the Si content increases, the size of the HfB_2 nanocrystals decreases from 50–60 nm down to 1–2 nm, the nanocrystals become randomly oriented and the fraction of the amorphous structure at the boundaries increases. This is consistent with the observed reduction in the residual stresses and increase in the high temperature oxidation resistance observed for these films.

© 2015 Elsevier B.V. All rights reserved.

1. Introduction

Nitride, boride and carbide based coatings of transition metals possess high potential for a wide-range of applications since they can combine a number of desirable properties (electric conductivity, high hardness, wear resistance and corrosion resistance at elevated temperatures). Special attention has been paid to Si–B–C–N [1–16], Ti–B–C [17–20], Ti–Si–B–C [21,22], Ti–B–C–N [17,20,21,23–36] and Zr–B–C–N [12,13,37–48] films. Recently, HfB_2-based thin films have attracted increasing interest due to their significantly higher oxidation resistance and much higher thermal conductivity of HfB_2 compared to TiB_2-based and ZrB_2-based materials [45,49–52]. These films are more promising candidates for applications involving high temperature environments, such as sharp leading edges for hypersonic vehicles, and propulsion systems. In addition, high thermal conductivity offers a number of advantages for high temperature applications, including improved thermal shock resistance and enhanced thermal radiation by efficient distribution of thermal energy over the available surfaces.

Very recently, Hf–B–Si–C films with different Si content have been fabricated using pulsed magnetron sputtering [53]. Variation of the Si fraction in these films has been found to result in tremendous differences in the hardness and oxidation resistance [53]. The Si-free Hf–B–C films exhibit a high hardness of 37 GPa, a high electrical conductivity (electrical resistivity of $1.8 \times 10^{-6}\ \Omega$ m) and a high compressive stress of 4.9 GPa. An addition of 2 at% Si in the film maintains hardness at about the same levels and decreases the compressive stress to 1.8 GPa. Further increase in the Si 9 at% retains a similar high hardness with a further reduction in the compressive stress but with significant improvement in the high temperature oxidation resistance. The Hf–B–Si–C films with 35 at% Si exhibit a reduction in hardness but the highest oxidation resistance in air

* Corresponding author.
E-mail address: meletis@uta.edu (E.I. Meletis).

http://dx.doi.org/10.1016/j.apsusc.2015.09.249
0169-4332/© 2015 Elsevier B.V. All rights reserved.

up to 800 °C. These films with such outstanding properties may be used as a new class of hard and electrically conductive protective coatings with a high oxidation resistance at elevated temperatures.

In this work, we have employed high-resolution transmission electron microscopy (HRTEM) and electron diffraction to study the effect of Si content (or, from another point of view, the effect of Si/[B+C] ratio – see the description of film preparation in Section 2.1) in the microstructural evolution of these films. The properties of the films have been reported in our previous study [53]. The motivation for this work was to develop an understanding of microstructure property relationship in these films as a function of the Si content.

2. Experimental details

2.1. Film preparation

The Hf–B–Si–C films were deposited in a Balzers BAS 450 PM sputtering system with a planar rectangular unbalanced magnetron and a stationary circular substrate holder (80 mm in diameter). The films were deposited on p-type Si (1 0 0) substrates using pulsed magnetron co-sputtering of Hf, B, Si and C from a single target (127 mm × 254 mm) in pure Ar gas. The single B_4C–Hf–Si target was prepared using a B_4C plate overlapped by Hf stripes with a fixed 15% Hf fraction and Si stripes with a varying 0–50% Si fraction in the target erosion area. Each of the Hf stripes constituted 5% of the target erosion area. Each of the Si stripes constituted 1–5% and exactly 5% of the target erosion area for Si fraction in the target erosion area 1–7.5% and 30%, respectively. The stripes were positioned on the target in order to achieve maximum homogeneity of the deposited films. A pulsed dc power supply (Rübig MP120) operating at an average target power of 500 W in a period with a fixed 85% duty cycle at a repetition frequency of 10 kHz was used to drive the magnetron. In order to reduce possible generation of internal stresses in the films, the substrates were at a floating potential. The crystallization was supported by an elevated temperature of 450 °C controlled by an infrared heater on the substrates during the deposition. The base pressure was 3×10^{-3} Pa and the argon pressure was 0.5 Pa with a constant Ar gas flow rate of approximately 25 sccm. The target to substrate distance was 100 mm. Four films were prepared with a Si fraction of 0%, 1%, 7.5% and 30% in the target erosion area having a composition in at% $Hf_{27}B_{57}C_8$, $Hf_{23}B_{55}Si_2C_{11}$, $Hf_{22}B_{54}Si_9C_9$ and $Hf_{21}B_{28}Si_{35}C_7$, respectively (without Zr contamination of the Hf stripes (0.5%), H (1%), O (2%) and Ar (5%)) [53]. The elemental composition of the films was determined by the Rutherford backscattering spectrometry (RBS) and the elastic recoil detection (ERD) methods [15].

2.2. Film characterization

The chemical composition of the films was investigated by X-ray photoelectron spectroscopy (XPS) on a Perkin-Elmer Phi 560 ESCA/SAM system and the spectra were acquired using a non-monochromated Al Kα excitation source. The Al Kα excitation is characteristic unresolved $K\alpha_{1,2}$ and has a characteristic energy of 1486.6 eV. Survey scans were conducted in the 0–600 eV range at 0.5 eV steps. The CasaXPS software was used for XPS spectra analysis and binding energy calibration was based on the C 1s peak at 284.5 eV. X-ray diffraction (XRD) θ–2θ measurements were conducted on a Bruker D8 Advance diffractometer using a Cu Kα (40 kV, 40 mA) radiation to study the crystallographic structure of the Hf–B–Si–C films. Films were scanned over the 2θ range from 10° to 60° with a scanning speed of 0.005°/s.

The microstructure of the films was studied by HRTEM. Selected-area electron diffraction patterns (SAED) and HRTEM images were recorded in a Hitachi H-9500 electron microscope operated at 300 kV with a point resolution of 0.18 nm. Cross-section and plan-view TEM specimens were prepared by the procedure of mechanical grinding, polishing and dimpling followed by Ar-ion milling using a Gatan model 691 precise ion polishing system (PIPS).

The residual stress in the films was determined from film curvature (measured by profilometry – Dektak 8 Stylus Profiler, Veeco) using the Stoney's formula.

3. Results and discussion

3.1. XPS analysis

Fig. 1(a) presents general XPS survey spectra of all four films. The spectra exhibit mainly the presence of Hf, Si, B, C and O (O and some of the C are from contamination). The results clearly show that the intensity of both Si 2p and Si 2s peaks increases with the Si fraction in the target erosion area. Fig. 1(b) shows the high-resolution XPS spectra and the associated deconvolution of the Si 2p peaks of all four Hf–B–Si–C films. The Si 2p peak for the $Hf_{23}B_{55}Si_2C_{11}$ film is very weak due to the small Si content and the binding energy (BE) of the Si 2p is roughly ∼101.7 eV. The BE of the Si 2p is ∼101 eV for the $Hf_{22}B_{54}Si_9C_9$ and ∼100.5 eV for the $Hf_{21}B_{28}Si_{35}C_7$ film indicating that the Si 2p peak shifts slightly to a lower binding energy position with the increase of the Si content. The Si 2p peaks for the $Hf_{22}B_{54}Si_9C_9$ and the $Hf_{21}B_{28}Si_{35}C_7$ films can be de-convoluted into two components **A** and **B** with a BE of 101.7 eV and 99.5 eV, respectively. The BE of component **B** is close to the Si 2p peak of hafnium silicide [55]. The BE of component **A** possibly corresponds to the Si 2p peak of the Si-B [56]. It is noted that increasing the Si content in the film results in the increase of component **B** and accordingly results in the Si 2p peak shifting to a lower BE position.

Fig. 1(c) shows the high-resolution XPS spectra and the associated deconvolution of the Hf 4f peaks of all four films presenting a BE of 16.4 eV, 16.0 eV, 15.5 eV and 14.5 eV for the $Hf_{27}B_{57}C_8$, $Hf_{23}B_{55}Si_2C_{11}$, $Hf_{22}B_{54}Si_9C_9$ and $Hf_{21}B_{28}Si_{35}C_7$ film, respectively. The BE of Hf 4f peak for the $Hf_{27}B_{57}C_8$ film is very close to that for HfB_2 (16.3 eV) reported in the literature [54]. The Hf 4f peaks for the $Hf_{23}B_{55}Si_2C_{11}$, $Hf_{22}B_{54}Si_9C_9$ and $Hf_{21}B_{28}Si_{35}C_7$ films can be de-convoluted into two components **C** and **D** with a BE of 16.4 eV and 14.6 eV, respectively. The latter one is closely equal to the BE of Hf 4f for hafnium silicide [55]. It clearly shows that increasing Si content in the films produces more **D** component (i.e., Hf—Si bonds) and accordingly lowers the BE of the Hf 4f resulting in the shift of the peak to a lower BE position.

Fig. 1(d) shows the high-resolution XPS spectra and the associated deconvolution of the B1s for $Hf_{27}B_{57}C_8$, $Hf_{23}B_{55}Si_2C_{11}$, $Hf_{22}B_{54}Si_9C_9$ and $Hf_{21}B_{28}Si_{35}C_7$ films. The B1s peak for the $Hf_{27}B_{57}C_8$ film can be de-convoluted into two components **E** (BE = 188.1 eV) and **F** (BE = 186.6 eV), which can be attributed to the B1s peak of Hf–B in HfB_2 [54] and that of B–C [61], respectively. The deconvolution of the B1s peak for the $Hf_{23}B_{55}Si_2C_{11}$, $Hf_{22}B_{54}Si_9C_9$ and $Hf_{21}B_{28}Si_{35}C_7$ films exhibit one more component **G** (BE = 186.9 eV) in addition to the components **E** and **F**. The BE of component G is close to that for B1s in B–Si (186.8 – 187.5 eV) [57]. The intensity of component G increases with the Si content in Hf–B–Si–C films indicating the increase of the amount of Si—B bonds and results in the observed downward shift of the peak.

3.2. XRD studies

We examined the crystal structure of the films using the θ–2θ XRD prior to conducting systematic TEM analysis (Fig. 2). XRD of the Si free $Hf_{27}B_{57}C_8$ film (0% Si) exhibit three diffraction peaks at 2θ angle of 25.28°, 41.95° and 51.98° corresponding to lattice spacing

Download English Version:

https://daneshyari.com/en/article/5356211

Download Persian Version:

https://daneshyari.com/article/5356211

Daneshyari.com